

---

# An Inpatient Comparison of $^{99m}\text{Tc}$ -EDDA/HYNIC-TOC with $^{111}\text{In}$ -DTPA-Octreotide for Diagnosis of Somatostatin Receptor-Expressing Tumors

Michael Gabriel, MD<sup>1</sup>; Clemens Decristoforo, PhD<sup>1</sup>; Eveline Donnemiller, MD<sup>1</sup>; Hanno Ulmer, PhD<sup>2</sup>; Christine Wafah Rychlinski, MD<sup>1</sup>; Stephen J. Mather, PhD<sup>3</sup>; and Roy Moncayo, MD<sup>1</sup>

<sup>1</sup>Department of Nuclear Medicine, University of Innsbruck, Innsbruck, Austria; <sup>2</sup>Institute of Biostatistics, University of Innsbruck, Innsbruck, Austria; and <sup>3</sup>Nuclear Medicine Research Laboratory, St. Bartholomew's Hospital, London, United Kingdom

The aim of this study was to compare the imaging abilities of the recently developed somatostatin analog,  $^{99m}\text{Tc}$ -hydrazinonicotinyl-Tyr<sup>3</sup>-octreotide ( $^{99m}\text{Tc}$ -HYNIC-TOC [ $^{99m}\text{Tc}$ -TOC]), with  $^{111}\text{In}$ -diethylenediaminepentaacetic acid-D-Phe<sup>1</sup>-octreotide ( $^{111}\text{In}$ -OCT [Octreoscan]) in patients undergoing routine somatostatin receptor (SSTR) scintigraphy. **Methods:** Forty-one patients (20 men, 21 women; age range, 29–75 y; mean age, 56.7 y) with either histologically proven or biologically and clinically suspected endocrine tumors were enrolled in the study. Four groups were distinguished: (a) patients being evaluated for the detection and localization of neuroendocrine tumors ( $n = 6$ ), (b) tumor staging ( $n = 19$ ), (c) patients being investigated to determine the SSTR status of tumor lesions ( $n = 11$ ), and (d) patient follow-up studies ( $n = 5$ ). Each patient received a mean activity of 150 MBq  $^{111}\text{In}$ -OCT and 350–400 MBq  $^{99m}\text{Tc}$ -TOC. Scintigraphy with  $^{99m}\text{Tc}$ -TOC was performed 4 h after injection and scintigraphy with  $^{111}\text{In}$ -OCT was performed 4 and 24 h after injection. SPECT studies of areas of interest were performed 4 h after injection for both tracers as well as at 24 h after injection for  $^{111}\text{In}$ -OCT. The time interval between the studies using each tracer ranged from 2 to 22 d (mean interval, 9.3 d). **Results:**  $^{111}\text{In}$ -OCT and  $^{99m}\text{Tc}$ -TOC showed an equivalent scan result in 32 patients (78%), 9 cases showed discrepancies (22%), false-negative results with  $^{111}\text{In}$ -OCT were seen in 6 cases (14.6%), whereas  $^{99m}\text{Tc}$ -TOC was false-positive in 2 cases (4.9%).  $^{111}\text{In}$ -OCT was true-negative in both cases. The false-positive findings of the  $^{99m}\text{Tc}$ -TOC studies were caused by nonspecific uptake in the bowel. In 1 case,  $^{99m}\text{Tc}$ -TOC correctly identified a metastasis in the lumbar spine but both scan results were false-positive because of an inflammatory process. In 21 patients with SSTR-expressing tumors, the semiquantitative region-of-interest analysis showed that  $^{99m}\text{Tc}$ -TOC achieved higher tumor-to-normal tissue ratios than  $^{111}\text{In}$ -OCT. **Conclusion:** This study revealed a higher sensitivity of  $^{99m}\text{Tc}$ -TOC as compared with  $^{111}\text{In}$ -OCT as an imaging agent for the localization of SSTR-expressing tumors. To avoid false-positive find-

ings with  $^{99m}\text{Tc}$ -OCT due to nonspecific tracer accumulation, additional scanning at 1–2 h after injection should be done.

**Key Words:**  $^{99m}\text{Tc}$ ; somatostatin; hydrazinonicotinic acid; tyrosine-octreotide; scintigraphy

**J Nucl Med 2003; 44:708–716**

---

**M**any human tumors are known to express somatostatin receptors (SSTRs) with varying intensity (1–8). Scintigraphy with the radiolabeled somatostatin analog  $^{111}\text{In}$ -diethylenediaminepentaacetic acid-D-Phe<sup>1</sup>-octreotide ( $^{111}\text{In}$ -OCT [Octreoscan; Mallinckrodt Medical, Petten, The Netherlands]) has gained acceptance as a diagnostic procedure for demonstrating neuroendocrine and other SSTR-positive tumors (9–13). However, this radiopharmaceutical has several drawbacks that are related to the use of  $^{111}\text{In}$  because this radiolabel has limited availability, high costs, and a medium  $\gamma$ -energy leading to suboptimal image resolution and relatively high radiation burden for the patient. We have recently described the development of a  $^{99m}\text{Tc}$ -labeled somatostatin analog, based on Tyr<sup>3</sup>-octreotide (TOC) and hydrazinonicotinic acid (HYNIC) as complexing ligand for  $^{99m}\text{Tc}$  (14). HYNIC-TOC can be labeled with  $^{99m}\text{Tc}$  using ethylenediamine *N,N'*-diacetic acid (EDDA) as coligand, resulting in a hydrophilic and stable complex,  $^{99m}\text{Tc}$ -EDDA/HYNIC-TOC ( $^{99m}\text{Tc}$ -TOC). In the initial study, the imaging characteristics of  $^{99m}\text{Tc}$ -TOC were compared with those of  $^{111}\text{In}$ -labeled octreotide analogs in 10 tumor patients (15). The pharmacokinetic properties of  $^{99m}\text{Tc}$ -TOC were found to be better than those of  $^{111}\text{In}$ -OCT. Higher target-to-nontarget ratios and higher absolute tumor uptake values were observed for  $^{99m}\text{Tc}$ -TOC and the optimal acquisition time for  $^{99m}\text{Tc}$ -TOC imaging was identified as 4 h after injection. The findings of this preliminary study indicated that  $^{99m}\text{Tc}$ -TOC is a promising candidate to replace  $^{111}\text{In}$ -OCT in diagnostic nuclear medicine. Besides these advan-

Received Sep. 23, 2002; revision accepted Jan. 13, 2003.

For correspondence or reprints contact: Clemens Decristoforo, PhD, Department of Nuclear Medicine, University of Innsbruck, Anichstrasse 35, A-6020 Innsbruck, Austria.

E-mail: clemens.decrisoforo@uibk.ac.at

tages, generator availability and improved image quality of  $^{99m}\text{Tc}$  over  $^{111}\text{In}$  make it a promising substance.

Clinical protocols for SSTR scintigraphy with  $^{111}\text{In}$ -OCT include imaging at 24 h after injection with additional imaging at 4 or 48 h after injection (13), whereas a  $^{99m}\text{Tc}$ -labeled analog cannot be used for scanning at such late time points. On the other hand, a single 1-d protocol with early imaging at 4 h after injection would improve patient compliance and simplify this important diagnostic procedure. The aim of our study was to evaluate the 2 radiopharmaceuticals in a larger series of patients routinely undergoing SSTR scintigraphy using a single-acquisition, 1-d protocol for  $^{99m}\text{Tc}$ -TOC as compared with the standard dual-time acquisition, 2-d protocol (4 and 24 h after injection) for  $^{111}\text{In}$ -OCT. Using a prospective cross-over study design, diagnostic efficacy and functional characteristics were compared in a study of sufficient size to be able to statistically compare the 2 radiopharmaceuticals.

## MATERIALS AND METHODS

### Patients

The clinical study was approved by the local ethical committee and all patients gave their informed consent before inclusion. Comparative scintigraphy with  $^{99m}\text{Tc}$ -TOC and  $^{111}\text{In}$ -OCT was performed on 41 patients (20 men, 21 women; age range, 29–75 y; mean age  $\pm$  SD,  $56.7 \pm 10.8$  y), details of which are given in Table 1. For analysis, the patients who were enrolled in this study were divided into 4 study groups (13). The first group (Detection;  $n = 6$ ) consisted of patients who underwent SSTR scintigraphy for the initial detection and localization of suspected neuroendocrine tumors and potential metastases. Patients with histologically proven endocrine malignancies were enrolled for staging in the second group (Staging;  $n = 19$ ). In the third group (SSTR status;  $n = 11$ ), the SSTR status of tumor lesions was evaluated for planning long-acting octreotide therapy. In the fourth group (Follow-up;  $n = 5$ ), follow-up was performed on patients after treatment of malignant disease to exclude or to detect tumor recurrence. The time interval between both studies ranged from 2 to 22 d (mean interval  $\pm$  SD,  $9.3 \pm 7.2$  d). Patients were not treated with unlabeled somatostatin analogs within 1 mo of the imaging studies being performed.

### Radiopharmaceuticals

$^{99m}\text{Tc}$ -TOC was prepared as described (14). Briefly, 20  $\mu\text{g}$  HYNIC-TOC were heated with 10 mg EDDA, 20 mg Tricine, 15  $\mu\text{g}$  stannous chloride dihydrate, and 1 GBq  $^{99m}\text{Tc}$ -pertechnetate in 2 mL of 0.05 mol/L phosphate buffer, pH 6, at 100°C for 10 min. The solution was purified using a Sep-Pak mini cartridge (Waters, Milford, MA) eluted with 80% ethanol and diluted with 5 mL saline. The purified radiolabeled peptide was sterilized by filtration, and 350–400 MBq of the resulting solution were used for each patient study. Radiochemical purity was >95% using analytic techniques based on high-performance liquid chromatography and thin-layer chromatography (TLC) as described elsewhere (16).

$^{111}\text{In}$ -OCT was prepared from a commercially available kit (Octreoscan; Mallinckrodt Medical). The injected dose per patient was 150 MBq. Radiochemical purity exceeded 95% analyzed by TLC using the recommended instant TLC method with 0.1 mol/L citrate buffer, pH 5, as solvent.

### Imaging

Whole-body imaging was performed with a double-head camera (Helix; Elscint, Haifa, Israel). For  $^{99m}\text{Tc}$  whole-body studies, the camera was equipped with a low-energy, all-purpose, parallel-hole collimator, window setting 140 keV, width 10%.  $^{111}\text{In}$  images were obtained using a medium- or high- energy, parallel-hole collimator, window setting over both  $^{111}\text{In}$  peaks at 172 and 246 keV with a window width of 20%. For  $^{99m}\text{Tc}$  tomographic acquisition, the same double-head gamma camera, as described above, was used. Acquisition parameters were 60 projections, 25 s per projection,  $64 \times 64$  matrix, and zoom, 1. SPECT of  $^{111}\text{In}$  scans was performed on a single-head camera (ZL3000; Siemens Medical Systems, Erlangen, Germany) equipped with a medium-energy, parallel-hole collimator using 60 projections, 35 s per projection, and  $64 \times 64$  matrix.  $^{99m}\text{Tc}$ -TOC studies were only performed 4 h after injection;  $^{111}\text{In}$ -OCT scintigraphy was performed 4 and 24 h after injection. In 5 (patients 8, 11, 13, 30, and 38) of 41 cases, patients were late for their schedule and could be imaged only 2–3 h after injection. In 3 cases (patients 6, 10, and 15), planar imaging of the abdomen was performed 48 h after injection to clarify doubtful findings. SPECT imaging of areas of interest was performed 4 h after injection and, for  $^{111}\text{In}$ -OCT, SPECT was also performed 24 h after injection. Abdominal SPECT was performed on 40 patients 4 and 24 h after injection with  $^{111}\text{In}$ -OCT and 4 h after injection with  $^{99m}\text{Tc}$ -TOC. In addition, SPECT of the chest was performed on 35 patients and SPECT of the head was performed on 14 patients 24 h after injection of  $^{111}\text{In}$ -OCT and 4 h after injection of  $^{99m}\text{Tc}$ -TOC. In patient 38, who was monitored after resection of a pituitary adenoma, only 1 SPECT study of the cerebrum 24 h after injection of  $^{111}\text{In}$ -OCT and 4 h after injection of  $^{99m}\text{Tc}$ -TOC was available. Because many SPECT acquisitions were performed, primarily for reasons of patient convenience, given the length of the procedure, complementary scintigraphic planar images were not acquired except delayed  $^{111}\text{In}$  images of the abdomen. For SPECT analysis, raw data were transferred to a HERMES system (Nuclear Diagnostics, London, U.K.) and filtered (Wiener filter) before reconstruction.

### CT and MRI

Abdominal, chest, and head CT scanning (HiSpeed Advantage CT scanner; General Electric Medical Systems, Milwaukee, WI) was performed with 5-mm contiguous sections using a  $512 \times 512$  matrix, before and after rapid intravenous infusion of contrast medium. All MRI examinations were performed on a 1.5-T whole-body scanner (Magnetom Vision; Siemens) by using a phased-array surface coil. T1- and T2-weighted spin-echo images were obtained with and without fat suppression.

### Image Analysis

Evaluation of each study was performed by independent visual interpretation by 2 nuclear medicine physicians who were experienced in the interpretation of  $^{111}\text{In}$ -OCT studies. The statistical design included a randomization of the sequence of the studies. Readers of the scans were unaware of the underlying pathology and the results of the standard staging procedures. Corresponding studies were compared for the final analysis lesion by lesion and ruled as matching or mismatching. Any focal tracer accumulation exceeding normal regional tracer uptake was rated as a pathologic finding (tumor uptake). Linear, nonfocal limited intestinal uptake was rated as nonspecific, nonpathologic uptake. In relevant areas, SPECT images were available to the viewer. All data were analyzed on a HERMES system using a region-of-interest (ROI)

**TABLE 1**  
Patient Characteristics

Patient no.	Sex	Age (y)	Pathology	Indication*	Interval† (d)	Confirmation
1	M	55	Papillary thyroid carcinoma	SSTR status	2	CT
2	F	55	Carcinoid syndrome	Detection	21	CT, MRI
3	M	67	GEP tumor	Follow-up	22	CT
4	F	39	Medullary thyroid carcinoma	SSTR status	3	CT
5	F	66	Small bowel carcinoid	Staging	2	CT
6	M	43	Small bowel carcinoid	Staging	2	CT
7	M	55	Ectopic Cushing syndrome	Detection	17	MRI, endoscopy
8	M	74	Papillary thyroid carcinoma	SSTR status	2	CT
9	F	51	Suspected gastrinoma	Detection	7	MRI, endoscopy
10	F	52	GEP tumor	Staging	2	CT
11	F	75	Follicular thyroid carcinoma	SSTR status	2	CT
12	M	58	Papillary thyroid carcinoma	SSTR status	2	CT
13	M	45	Paraganglioma	Follow-up	19	CT
14	F	66	Papillary thyroid carcinoma	SSTR status	11	CT, biopsy
15	F	64	Suspected gastrinoma	Detection	15	CT, endoscopy
16	M	41	Islet cell tumor	Staging	19	CT
17	F	62	Carcinoid of papilla of Vater	Staging	2	CT
18	M	66	Medullary thyroid carcinoma	Staging	2	CT, MRI
19	M	67	Medullary thyroid carcinoma	SSTR status	2	CT
20	M	56	Follicular thyroid carcinoma	SSTR status	3	CT
21	F	58	Bronchogenic carcinoid	SSTR status	6	CT, biopsy
22	F	75	Follicular thyroid carcinoma	SSTR status	8	CT
23	M	51	Small bowel carcinoid	Staging	5	CT, endoscopy
24	F	47	GEP tumor	Staging	22	CT
25	M	63	GEP tumor	Staging	19	CT
26	F	39	GEP tumor	Staging	11	CT
27	M	55	Small bowel carcinoid	Staging	4	CT, MRI
28	M	56	GEP tumor	Staging	13	CT
29	M	53	Suspected gastrinoma	Detection	17	CT, endoscopy
30	F	29	Carcinoid of appendix	Follow-up	12	CT
31	M	64	Follicular thyroid carcinoma	SSTR status	2	CT
32	F	58	GEP tumor	Staging	10	CT
33	F	65	Carcinoid syndrome	Detection	5	CT, endoscopy
34	F	69	Small bowel carcinoid	Follow-up	10	CT, endoscopy
35	F	68	GEP tumor	Staging	21	CT, second look
36	F	50	Carcinoid of rectum	Staging	11	CT
37	M	45	Carcinoid of pancreas	Staging	14	CT
38	F	54	Pituitary adenoma	Follow-up	2	MRI, biopsy
39	M	53	Small bowel carcinoid	Staging	9	CT, MRI
40	M	71	Small bowel carcinoid	Staging	22	CT
41	F	46	GEP tumor	Staging	2	CT

\*Detection = detection and localization of suspected neuroendocrine tumors and their metastases; Staging = staging patients with neuroendocrine tumors; SSTR status = determination of SSTR status; Follow-up = follow-up studies after successful therapy.

†Time interval between both studies.

GEP tumor = (nonfunctioning) neuroendocrine gastroenteropancreatic tumor.

technique for semiquantitative analysis of major organ and tumor uptake. ROIs were drawn over the whole body, sites of tumor uptake, kidney, liver, spleen, heart, and a right thigh area (as an ROI for muscle) on both the anterior and the posterior whole-body views of the <sup>111</sup>In and <sup>99m</sup>Tc images. For evaluation of kidney uptake, the left kidney was selected to avoid interference from liver superimposition. Parts of organs showing tumor infiltration or superimposition were excluded from evaluation of organ uptake. Total counts and counts/pixel in all ROIs were calculated. For the evaluation of uptake in malignant tissue, the lesion with the maximum uptake in counts/pixel was selected and tumor-to-organ ratios for this lesion were calculated from the respective counts/

pixel values in normal organs. The projection with the highest tumor-to-organ ratios was selected (anterior or posterior) and used for a direct comparison between <sup>111</sup>In-OCT and <sup>99m</sup>Tc-TOC in the same patient.

Because not all lesions could be histologically assessed and the different imaging procedures frequently showed discrepancies, the consensus was based on the sum of all conventional imaging procedures excluding scintigraphic data. For evaluation of previously unconfirmed scintigraphic abnormalities, 3 mo after the scans, repeated clinical examinations with CT or MRI of the abdomen, chest, and neck were performed. So far, all patients underwent imaging with either CT (*n* = 34), MRI (*n* = 3), or both

**TABLE 2**  
Scintigraphic Results of <sup>99m</sup>Tc-TOC and <sup>111</sup>In-OCT: Analysis per Lesion

Group	n	<sup>99m</sup> Tc-TOC				<sup>111</sup> In-OCT			
		TP	TN	FP	FN	TP	TN	FP	FN
Detection	6	0	0	1	5	0	1	0	5
Staging	84	78	0	1	5	67	0	1	16
SSTR status	29	21	0	0	8	20	0	0	9
Follow-up	6	3	2	1	0	3	3	0	0
Overall	125	102	2	3	18	90	4	1	30

TP = true-positive; TN = true-negative; FP = false-positive; FN = false-negative.

modalities ( $n = 4$ ). CT and MR scans were interpreted by experienced radiologists who were unaware of the scintigraphic result. A positive diagnosis was based on the specific appearance of malignant disease derived from neuroendocrine tumors as described elsewhere (17). If the clinical setting required further information, endoscopic procedures (e.g., colonoscopy and second-look surgery) were also performed. Attention has been directed at still unproven findings of the scans.

### Statistical Analysis

For statistical analysis the tumor-to-organ ratios were expressed as medians and ranges. Paired  $t$  tests and Wilcoxon tests were used to determine statistically significant differences in the semiquantitative analyses of the groups, as appropriate. The McNemar test of correlated properties was used to statistically compare the scintigraphic results of <sup>99m</sup>Tc-TOC and <sup>111</sup>In-OCT. Analysis was done on a lesion basis and on a patient basis. Two-sided  $P$  values  $< 0.05$  were considered significant. Cohen's  $\kappa$  with confidence intervals of 95% was calculated to show the degree of association between the 2 techniques. A randomization procedure was used for determination of the order of the studies being evaluated.

### RESULTS

Analysis per lesion from scintigraphy of all 41 patients studied are summarized in Table 2. Results per patient are reported in Table 3. True-positive results were obtained in 27 patients with <sup>99m</sup>Tc-TOC (65.9%) and in 21 patients with <sup>111</sup>In-OCT (51.2%). In 11 cases (26.8%) scintigraphy was negative with <sup>99m</sup>Tc-TOC and in 19 cases it was negative (46.4%) with <sup>111</sup>In-OCT. Of the 11 negative scintigraphic

studies using <sup>99m</sup>Tc-TOC in 9 patients (21.9%), pathologic findings were detected on the basis of conventional procedures, whereas <sup>111</sup>In-OCT was false-negative in 15 cases (36.6%). In 3 patients (7.3%) a false-positive scan result was obtained with <sup>99m</sup>Tc-TOC, whereas <sup>111</sup>In-OCT was false-positive in only 1 case. Overall, <sup>99m</sup>Tc-TOC and <sup>111</sup>In-OCT scintigraphy produced total agreement in 32 cases (78.1%). In 11 patients (26.8%) no findings suggestive of abnormal pathology were detected in both studies. This group included 5 patients (12.2%) who were investigated for localization of a suspected neuroendocrine tumor, in 1 patient (2.4%) tumor staging was performed, SSTR status was undertaken in 3 patients (7.3%), and in 2 patients (4.9%) a suspected recurrence was excluded by SSTR scintigraphy after successful therapy. In the remaining 30 patients (73.2%), at least 1 scintigraphic study (<sup>99m</sup>Tc-TOC or <sup>111</sup>In-OCT) revealed scintigraphic abnormalities. Overall, 105 hot spots were detected with <sup>99m</sup>Tc-TOC, whereas <sup>111</sup>In-OCT found 91. Site-related findings are listed in Figure 1.

In 21 patients (51.2%) true-positive findings were observed with both tracers, leading to an equivalent scan result (Fig. 2). Of these 21 patients 12 (29.3%) had been referred for tumor staging, 7 (17.1%) were under investigation to determine the SSTR status, and follow-up was being performed in 2 patients. There was 1 false-positive finding in both studies (patient 18). This patient (underwent surgery for a medullary thyroid carcinoma) presented with an elevated serum calcitonin level. In both studies enhanced tracer accumulation was shown in the right hip, so that a bone

**TABLE 3**  
Scintigraphic Results of <sup>99m</sup>Tc-TOC and <sup>111</sup>In-OCT: Analysis per Patient

Group	n	<sup>99m</sup> Tc-TOC				<sup>111</sup> In-OCT			
		TP	TN	FP	FN	TP	TN	FP	FN
Detection	6	0	0	1	5	0	1	0	5
Staging	19	17	0	1	1	12	0	1	6
SSTR status	11	8	0	0	3	7	0	0	4
Follow-up	5	2	2	1	0	2	3	0	0
Overall	41	27	2	3	9	21	4	1	15

TP = true-positive; TN = true-negative; FP = false-positive; FN = false-negative.

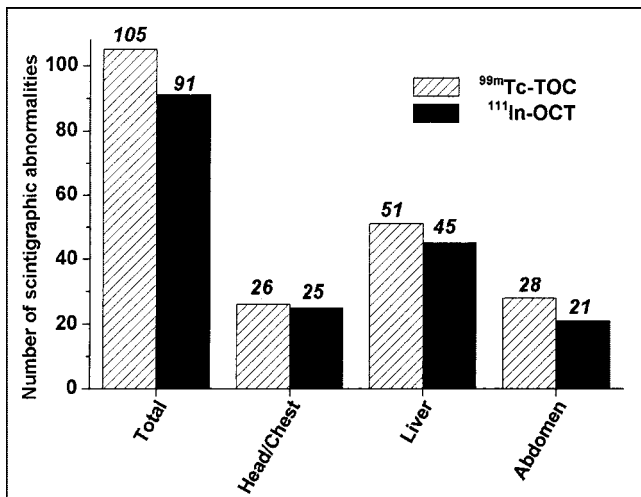


**FIGURE 1.** Number of abnormal findings revealed by <sup>99m</sup>Tc-TOC and <sup>111</sup>In-OCT in 31 patients.

metastasis could not be excluded. Other radiologic imaging modalities, including CT and MRI, confirmed arthritis of the hip. In the same patient an SSTR-expressing metastasis in the upper lumbar spine was poorly depicted on <sup>99m</sup>Tc-TOC scintigraphy but was confirmed by MRI. This focus was not visualized with <sup>111</sup>In-OCT. However, this case was classified as false-positive for both studies in Table 3. Discrepancies between the 2 studies were observed in a further 8 patients (19.5%; patients 6, 14, 17, 25, 27, 29, 34, and 35). A suspicious finding in the upper part of the abdomen was detected with the <sup>99m</sup>Tc-TOC scan in patient 29, who presented with a slightly elevated serum gastrin level and clinical signs of a gastrinoma. This abdominal focus could not be delineated on the <sup>111</sup>In-OCT scan. This patient also suffered from a high-grade non-Hodgkin's lymphoma of the small bowel but was in complete remission after 5 cycles of cyclophosphamide, hydroxydaunomycin, oncovin, and prednisone at the time of the scans. <sup>18</sup>F-FDG PET, CT, and endoscopy were negative and several serum gastrin assays did not show any significant change during 9 mo of follow-up. This <sup>99m</sup>Tc-TOC study was, therefore, considered false-positive. Five patients (12.2%) who were being evaluated for tumor staging showed discrepant scan results (patients 6, 17, 25, 27, and 35). Patient 17 had a carcinoid of the papilla of Vater and 2 metastases in the liver that were positive on both studies. The <sup>99m</sup>Tc-TOC scan detected an additional retroperitoneal lymph node metastasis that was confirmed by CT. In patient 27, <sup>111</sup>In-OCT was negative for a solitary liver metastasis after the surgical removal of a small bowel carcinoid, whereas <sup>99m</sup>Tc-TOC was positive. This result was confirmed by MRI.

In the remaining 3 cases of this group, further clinical management was influenced by positive findings on the <sup>99m</sup>Tc-TOC scan. In patient 6, with hepatic metastases due to a small bowel carcinoid, <sup>99m</sup>Tc-TOC scintigraphy additionally showed 2 paraaortal lymph node metastases in the

abdomen that were confirmed by CT 3 mo later. In patient 35, with a neuroendocrine tumor of the tail of the pancreas, a solitary metastasis of the liver was distinctly delineated with <sup>111</sup>In-OCT as well as with <sup>99m</sup>Tc-TOC. However, a small residual tumor in projection to the cranial pole of the left kidney was visualized only by <sup>99m</sup>Tc-TOC. A second-look procedure confirmed this finding. Both patients were spared from extensive surgical intervention to remove liver metastases.

In patient 25, who suffered from a neuroendocrine tumor of the pancreas with multiple liver metastases, <sup>99m</sup>Tc-TOC scintigraphy showed 3 small metastases in the right liver lobe and 2 small metastases in the left liver lobe, all of which were in the range of 1.0 cm. Although the <sup>111</sup>In-OCT scan showed a patchy pattern of uptake in the liver, the metastases could not be delineated. All findings were confirmed by CT. This patient was subsequently treated with <sup>90</sup>Y-dodecanetetraacetic acid (DOTA)-TOC leading to partial remission.

The treatment regime was also adapted in patient 14, who was referred to our department to determine the SSTR status of a solitary pulmonary metastasis of a papillary carcinoma of the thyroid gland. Radioiodine uptake was negative. CT-controlled biopsy of the lung lesion confirmed the thyroid carcinoma origin of the metastasis. On planar whole-body views as well as on SPECT, <sup>99m</sup>Tc-TOC showed an enhanced tracer accumulation in this lesion, whereas the <sup>111</sup>In-OCT scan was negative (Fig. 3). The size of this metastasis was 1.3 × 1.4 cm. Because the patient refused further surgical intervention we started a treatment regime using a long-acting SST analog. Follow-up during 8 mo showed a slight increase in serum thyroglobulin but the lung metastasis did not show an increase in size.

Another discrepant scan result was found in patient 34, who was investigated to exclude recurrence of a secretory inactive neuroendocrine tumor of the small bowel. A soli-

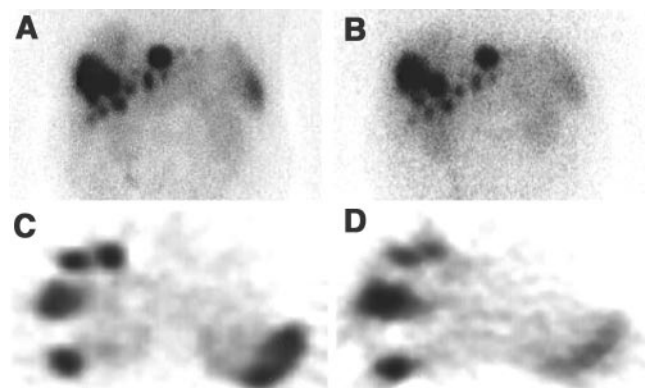


**FIGURE 2.** A 51-y-old man (patient 23) with multiple liver metastases of small bowel carcinoid. Matching tracer accumulations are shown by <sup>99m</sup>Tc-TOC and <sup>111</sup>In-OCT on anterior views (<sup>99m</sup>Tc-TOC 4 h after injection [A] and <sup>111</sup>In-OCT 24 h after injection [B]) as well as on SPECT (<sup>99m</sup>Tc-TOC 4 h after injection [C] and <sup>111</sup>In-OCT 24 h after injection [D]).

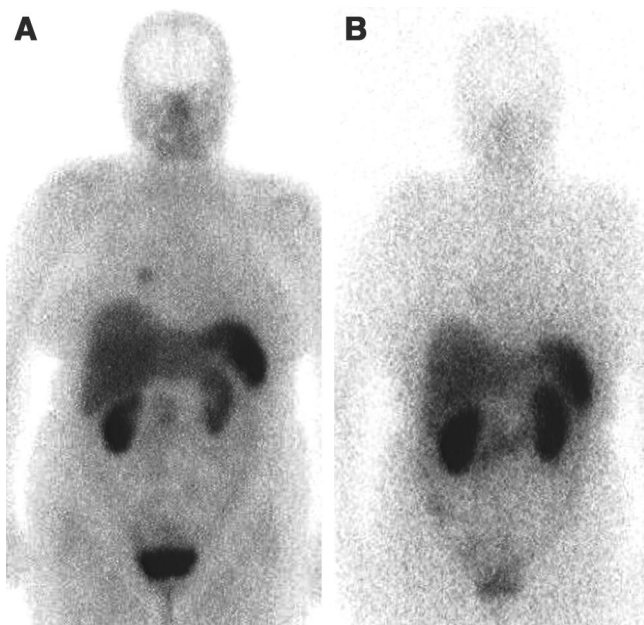


**FIGURE 3.** A 66-y-old woman (patient 14) with papillary thyroid cancer. SSTR scintigraphy with  $^{99m}\text{Tc}$ -TOC (A) shows clear uptake in solitary metastasis in right lung.  $^{111}\text{In}$ -OCT scan was negative 4 and 24 h after injection (B).

tary focus was shown in projection to the small bowel on the right side with  $^{99m}\text{Tc}$ -TOC, whereas  $^{111}\text{In}$ -OCT was negative (Fig. 4). The  $^{99m}\text{Tc}$ -TOC finding could not be confirmed by repeated CT and an endoscopic procedure was also negative. This  $^{99m}\text{Tc}$ -TOC study was, therefore, considered false-positive.

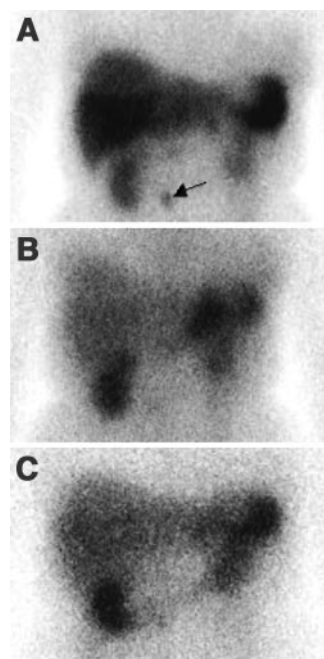
The delayed planar  $^{111}\text{In}$  images of the abdomen did not change the scan results in each of these 3 cases (patients 6, 10, and 15).

Figure 5 shows a summary of the semiquantitative ROI analyses from 21 patients with SSTR-expressing tumors and a matching  $^{111}\text{In}$ -OCT/ $^{99m}\text{Tc}$ -TOC scan result. In the images 4 h after injection, tumor-to-organ ratios obtained with  $^{99m}\text{Tc}$ -TOC were higher than those obtained with  $^{111}\text{In}$ -OCT in all organs except the spleen. These differences were statistically significant ( $P < 0.001$ ) for tumor-to-blood, tumor-to-liver, and tumor-to-kidney ratios. When 24-h  $^{111}\text{In}$ -OCT images were compared with 4-h  $^{99m}\text{Tc}$ -TOC images, only the tumor-to-kidney ratios were statistically significant, with  $^{99m}\text{Tc}$ -TOC again showing superior ratios.

From the clinical point of view,  $^{99m}\text{Tc}$ -TOC showed statistically significant better results in terms of detection and localization of pathologic sites ( $P < 0.001$ ) using the McNemar test, and Cohen's  $\kappa$  of 0.68 (0.52–0.83) revealed a moderate association between both techniques. An analysis per patient comparing the scan results emphasizes the improved diagnostic efficacy of  $^{99m}\text{Tc}$ -TOC with a  $P$  value of 0.0078 and Cohen's  $\kappa$  of 0.6 (0.37–0.83). The correlation coefficient was based on 41 observations.

## DISCUSSION

Since the introduction of SSTR imaging in 1989 (18), scintigraphy with  $^{111}\text{In}$ -OCT has become a reliable, noninvasive method for diagnosing different SSTR-expressing tumors with several clinical implications (9,19–27). More recently, researchers have tried to develop  $^{99m}\text{Tc}$ -labeled somatostatin analogs to improve availability and image quality of SSTR scintigraphy as well as to reduce the radiation burden to the patient (28,29). Only 1 analog,  $^{99m}\text{Tc}$ -depreotide (P829 [NeoTECT; Amersham Health, Amersham, U.K.]), has so far been commercially introduced into clinical practice (30). However, this compound does not have imaging properties similar to those of  $^{111}\text{In}$ -OCT. Although it has proven sufficient diagnostic efficacy in the evaluation of thoracic nodules (31,32), the detection rate for  $^{99m}\text{Tc}$ -P829 scintigraphy in patients with endocrine tumors was lower than that of  $^{111}\text{In}$ -OCT scintigraphy (33).  $^{99m}\text{Tc}$ -TOC, based on an octreotide derivative, is a new compound that performed somewhat better than  $^{111}\text{In}$ -OCT in a pilot study done on 10 patients (15). In this study with 41 patients, these initial findings were confirmed not only by qualitative but also by semiquantitative image analysis. Altogether, no side effects were observed after intravenous injection ( $n = 51$ ). Unlike NeoTECT, only minimal hepatobiliary clearance of  $^{99m}\text{Tc}$ -TOC was observed. Although the kidneys are the predominant excretion organs for both  $^{99m}\text{Tc}$ -TOC and  $^{111}\text{In}$ -OCT, significantly higher tumor-to-



**FIGURE 4.** A 69-y-old woman (patient 34) monitored 2 y after surgical treatment of small bowel carcinoid. On  $^{99m}\text{Tc}$ -TOC scan, focal uptake (A), highly suspicious for tumor recurrence, was observed in abdomen (arrow).  $^{111}\text{In}$ -OCT images were negative at 4 h (B) and 24 h (C) after injection. Further investigations could not confirm this abnormal finding;  $^{99m}\text{Tc}$ -TOC scan result was considered false.

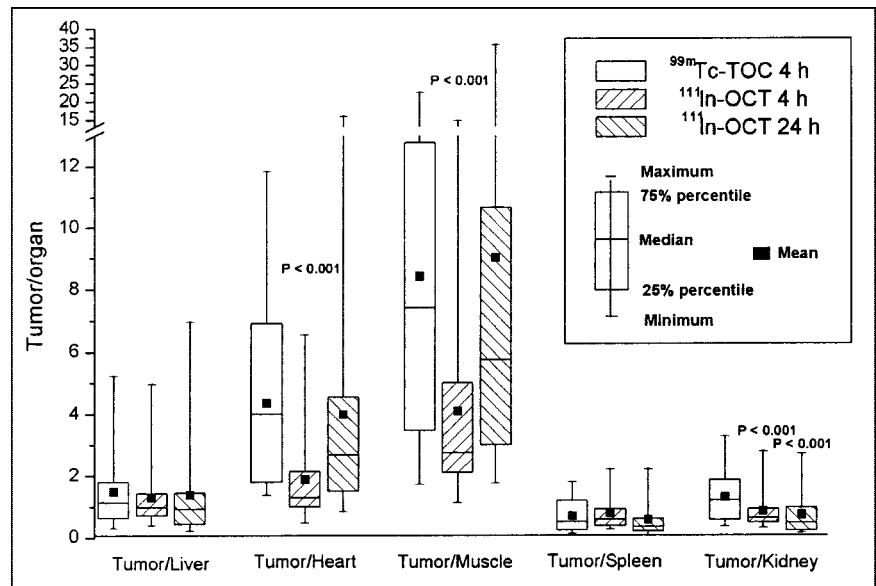


**FIGURE 5.** Statistical analysis of tumor-to-organ ratios in matching studies with pathologic uptake ( $n = 21$ ).

kidney ratios were obtained on the 4-h  $^{99m}\text{Tc}$ -TOC images as compared with the 4- or 24-h  $^{111}\text{In}$ -OCT images. These results indicate that the advantage of the longer half-life of  $^{111}\text{In}$ , with potential imaging up to 48 h after injection, were compensated by the higher spatial resolution of  $^{99m}\text{Tc}$ , better counting statistics, and the higher tumor uptake of  $^{99m}\text{Tc}$ -TOC.

In this series of patients, the clinical information obtained with  $^{99m}\text{Tc}$ -TOC using a 1-d, single-acquisition, 4-h after-injection protocol was at least comparable to the standard 2-d protocol of  $^{111}\text{In}$ -OCT and no advantage was gained from delayed imaging with the longer-lived radionuclide. However, in 9 of 41 patients, differences were observed between the 2 radiopharmaceuticals. In all of these cases, additional hot spots were detected on the  $^{99m}\text{Tc}$ -TOC scans. This higher sensitivity was statistically significant according to the McNemar test of correlated properties. However, the use of  $^{99m}\text{Tc}$ -TOC also resulted in a greater number of false-positive results. Despite a rapid background clearance and low hepatobiliary excretion, some nonspecific accumulation in the bowel can lead to false-positive interpretations with  $^{99m}\text{Tc}$ -TOC when a single-acquisition protocol is used. This phenomenon was observed in 2 patients (patients 29 and 34). If the area of clinical interest is in the abdomen (e.g., staging of neuroendocrine gastroenteropancreatic tumors), additional imaging 1–2 h after injection could avoid such pitfalls, because the favorable pharmacokinetics allows accurate imaging at such early time points (15). Adequate bowel preparation, which can be advantageous for investigations with  $^{111}\text{In}$ -OCT, cannot be used to improve accuracy of the  $^{99m}\text{Tc}$  studies considering the short time range available between tracer application and scanning.

Although  $^{111}\text{In}$ -OCT scintigraphy, especially with SPECT, can often provide additional valuable staging in-

formation when compared with other imaging modalities (34,35,36), some sites of metastases will be missed (37). In our study, the use of  $^{111}\text{In}$ -OCT resulted in 6 false-negative cases in which  $^{99m}\text{Tc}$ -TOC was true-positive. In some of these cases, this higher sensitivity of  $^{99m}\text{Tc}$ -TOC even resulted in a change of patient management. When taking into account the high number of false-negative results with  $^{111}\text{In}$ -OCT, we feel that the potential advantage of  $^{111}\text{In}$ -OCT with acquisition at later time points was compensated by the advantage of improved pharmacokinetics allowing earlier imaging with  $^{99m}\text{Tc}$ -TOC.

Receptor-specific accumulation in the thyroid gland regularly resulted in a clearer delineation of this organ on the  $^{99m}\text{Tc}$ -TOC study than on the  $^{111}\text{In}$ -OCT scan, even in the absence of thyroid disease. Uptake of free technetium-pertechnetate could be excluded because the amount of free pertechnetate present (as determined by HPLC) was  $<1\%$  and no uptake was shown in stomach or salivary glands. This suggests that  $^{99m}\text{Tc}$ -TOC may show advantages over  $^{111}\text{In}$ -OCT not only in the visualization of smaller lesions but also of lesions with a lower density of SSTRs, such as in thyroid tumors (38). In our series we studied 8 patients with differentiated nonmedullary thyroid cancer and 3 patients with medullary thyroid cancer. In these 11 patients,  $^{99m}\text{Tc}$ -TOC and  $^{111}\text{In}$ -OCT showed equivalent scan results in 10 cases. However, in 1 patient (patient 14), with a papillary thyroid carcinoma showing a solitary radioiodine-negative metastasis in the right lung, tracer uptake was clearly visualized with  $^{99m}\text{Tc}$ -TOC, whereas  $^{111}\text{In}$ -OCT was negative (Fig. 3), which formed the basis for treatment with an unlabeled SST analog.

This patient and another patient (patient 25), with multiple SSTR-expressing liver metastases on  $^{99m}\text{Tc}$ -TOC, negative on  $^{111}\text{In}$ -OCT, who was successfully treated with  $^{90}\text{Y}$ -DOTA-TOC, demonstrate that a greater number of patients

might benefit from an improved in vivo detection of SSTR-expressing tumor tissue. Patients who exhibit a positive scan result are, in principle, accessible to treatment options with either unlabeled SST analogs or analogs labeled with  $\beta^-$ -emitting isotopes. Improved diagnostic accuracy might therefore also help to encourage new clinical applications for SSTR scintigraphy. The lower radiation dose received with  $^{99m}\text{Tc}$  favors the use of repeated investigations—for example, for therapeutic monitoring or applications in children. The physical decay characteristics of  $^{99m}\text{Tc}$  might also improve the use of surgical probes for detection of involved lymph nodes (39). In this series of patients several different kinds of tumor types and clinical indications were included. Although this study proves that  $^{99m}\text{Tc}$ -TOC could be an alternative to the clinical use of  $^{111}\text{In}$ -OCT, further phase III trials are still necessary to assess the value of  $^{99m}\text{Tc}$ -TOC in clinical nuclear medicine. Further improvements in SSTR scintigraphy are ongoing. Other  $^{99m}\text{Tc}$ -labeled analogs have been developed using tetraamine-functionalized Tyr<sup>3</sup>-octreotate. Such analogs are expected to show even higher affinity for SSTR subtype 2 (7). Promising preclinical results have already demonstrated favorable pharmacokinetics and very high tumor uptake (40).

## CONCLUSION

This study shows that the use of a single-acquisition protocol with  $^{99m}\text{Tc}$ -TOC can provide improved clinical information when compared with a 2-d  $^{111}\text{In}$ -OCT protocol.  $^{99m}\text{Tc}$ -TOC combines the advantages of favorable pharmacokinetics, higher spatial resolution, lower radiation dose, and improved availability of  $^{99m}\text{Tc}$  with a simplified imaging procedure and could replace  $^{111}\text{In}$ -OCT for routine SSTR scintigraphy. Further clinical studies are required to assess the usefulness of  $^{99m}\text{Tc}$ -TOC in more specific clinical settings.

## REFERENCES

1. Reubi JC, Häcki WH, Lamberts SWJ. Hormones producing gastrointestinal tumors contain a high density of somatostatin receptors. *J Clin Endocrinol Metab.* 1987;65:1127–1134.
2. Reubi JC, Kvolts L, Krenning EP, Lamberts SWJ. Distribution of somatostatin receptor in normal and tumour tissue. *Metabolism.* 1990;30(suppl 2):78–81.
3. Reubi JC, Kvolts L, Krenning E, Lamberts SW. In vivo and in vitro detection of somatostatin receptors in human malignant tissues. *Acta Oncol.* 1991;30:463–468.
4. Reubi JC, Krenning E, Lamberts SW, Kvolts L. In vitro detection of somatostatin receptors in human tumors. *Digestion.* 1993;54:76–83.
5. Reubi JC, Schaefer JC, Markwalder R, Waser B, Horisberger U, Laissue J. Distribution of somatostatin receptors in normal and neoplastic human tissues: recent advances and potential relevance. *Yale J Biol Med.* 1997;70:471–479.
6. Hofland LJ, Liu Q, Van Koetsveld PM, et al. Immunohistochemical detection of somatostatin receptor subtypes sst1 and sst2A in human somatostatin receptor positive tumors. *J Clin Endocrinol Metab.* 1999;84:775–780.
7. Reubi JC, Schar JC, Waser B, et al. Affinity profiles for human somatostatin receptor subtypes SST1-SST5 of somatostatin radiotracers selected for scintigraphic and radiotherapeutic use. *Eur J Nucl Med.* 2000;27:237–282.
8. Reubi JC, Waser B, Schaefer JC, Laissue JA. Somatostatin receptor sst1-sst5 expression in normal and neoplastic human tissues using receptor autoradiography with subtype-selective ligands. *Eur J Nucl Med.* 2001;28:836–846.
9. Krenning EP, Kwekkeboom DJ, Bakker WH, et al. Somatostatin receptor scintigraphy with [111-In-DTPA-D-Phe] and [123-I-tyr]-octreotide: the Rotterdam experience with more than 1000 patients. *Eur J Nucl Med.* 1993;20:716–731.

10. Krenning EP, Kwekkeboom DJ, de Jong M, et al. Essentials of peptide receptor scintigraphy with emphasis on somatostatin analog octreotide. *Semin Oncol.* 1994;21(suppl 13):6–14.
11. Lamberts SWJ, Reubi JC, Krenning EP. Somatostatin and the concept of peptide receptor scintigraphy in oncology. *Semin Oncol.* 1994;21(suppl 13):1–5.
12. Kwekkeboom D, Krenning EP, de Jong M. Peptide receptor imaging and therapy. *J Nucl Med.* 2000;41:1704–1713.
13. Balon HR, Goldsmith SJ, Siegel BA, et al. Procedure guidelines for somatostatin receptor scintigraphy with  $^{111}\text{In}$ -pentetreotide. *J Nucl Med.* 2001;42:1134–1138.
14. Decristoforo C, Melendez-Alafort L, Sosabowski JK, Mather SJ.  $^{99m}\text{Tc}$ -HYNIC-[Tyr<sup>3</sup>]-octreotide for imaging somatostatin-receptor-positive tumors: preclinical evaluation and comparison with  $^{111}\text{In}$ -octreotide. *J Nucl Med.* 2000;41:1114–1119.
15. Decristoforo C, Mather SJ, Cholewinski W, Donnemiller E, Riccabona G, Moncayo R.  $^{99m}\text{Tc}$ -EDDA/HYNIC-TOC: a new  $^{99m}\text{Tc}$ -labelled radiopharmaceutical for imaging somatostatin receptor-positive tumours: first clinical results and intra-patient comparison with  $^{111}\text{In}$ -labelled octreotide derivatives. *Eur J Nucl Med.* 2000;27:1318–1325.
16. Decristoforo C, Mather SJ. Preparation,  $^{99m}\text{Tc}$ -labelling and in vitro characterisation of HYNIC and N<sub>5</sub>S modified RC-160 and [Tyr<sup>3</sup>]-octreotide. *Bioconjug Chem.* 1999;10:431–438.
17. Debray MP, Geoffroy O, Laissy JP, et al. Imaging appearances of metastases from neuroendocrine tumours of the pancreas. *Br J Radiol.* 2001;74:1065–1070.
18. Krenning EP, Bakker WH, Breeman WA, et al. Localisation of endocrine-related tumours with radioiodinated analogue of somatostatin. *Lancet.* 1989;333:242–244.
19. Lamberts SWJ, Hofland LJ, Van Koetsveld PM, et al. Parallel in vivo and in vitro detection of functional somatostatin receptors in human pancreatic tumors: consequences with regard to diagnosis, localization, and therapy. *J Clin Endocrinol Metab.* 1990;71:566–574.
20. Lamberts SWJ, Krenning EP, Reubi JC. The role of somatostatin and its analogs in the diagnosis and treatment of tumors. *Endocr Rev.* 1991;12:450–482.
21. Pauwels S, Leners N, Fiasse R, et al. Localization of gastroenteropancreatic tumors with  $^{111}\text{In}$  indium pentetreotide scintigraphy. *Semin Oncol.* 1994;21:15–20.
22. Zimmer T, Ziegler K, Bader M, et al. Localization of neuroendocrine tumours of the upper gastrointestinal tract. *Gut.* 1994;35:471–475.
23. Rieger A, Rainov NG, Elfrich C, et al. Somatostatin receptor scintigraphy in patients with pituitary adenoma. *Neurosurg Rev.* 1997;20:7–12.
24. Alexander HR, Fraker DL, Norton JA, et al. Prospective study of somatostatin receptor scintigraphy and its effect on operative outcome in patients with Zollinger-Ellison syndrome. *Ann Surg.* 1998;228:228–238.
25. Berna L, Chico A, Matias-Guiu X, et al. Use of somatostatin analogue scintigraphy in the localization of recurrent medullary thyroid carcinoma. *Eur J Nucl Med.* 1998;25:1482–1488.
26. Telischi EF, Bustillo A, Whiteman ML, et al. Octreotide scintigraphy for the detection of paragangliomas. *Otolaryngol Head Neck Surg.* 2000;122:358–362.
27. Haslinghuis LM, Krenning EP, De Herder WW, Reijs AE, Kwekkeboom DJ. Somatostatin receptor scintigraphy in the follow-up of patients with differentiated thyroid cancer. *J Endocrinol Invest.* 2001;24:415–422.
28. Maina T, Stolz B, Albert R, Bruns C, Koch P, Macke H. Synthesis, radiochemistry and biological evaluation of a new somatostatin analogue (SDZ 219-387) labelled with technetium-99m. *Eur J Nucl Med.* 1994;21:437–444.
29. Kolan H, Li J, Thakur ML. Sandostatin labeled with  $^{99m}\text{Tc}$ : in vitro stability, in vivo validity and comparison with  $^{111}\text{In}$ -DTPA-octreotide. *Pept Res.* 1996;9:144–150.
30. Vallabhajosula S, Moyer BR, Lister-James J, et al. Preclinical evaluation of technetium-99m-labeled somatostatin receptor-binding peptides. *J Nucl Med.* 1996;37:1016–1022.
31. Blum JE, Handmaker H, Rinne NA. The utility of a somatostatin-type receptor binding peptide radiopharmaceutical (P829) in the evaluation of solitary pulmonary nodules. *Chest.* 1999;115:224–232.
32. Menda Y, Kahn D. Somatostatin receptor imaging of non-small cell lung cancer with  $^{99m}\text{Tc}$  depreotide. *Semin Nucl Med.* 2002;32:92–96.
33. Lebtahi R, Le Cloirec J, Houzard C, et al. Detection of neuroendocrine tumors:  $^{99m}\text{Tc}$ -P829 scintigraphy compared with  $^{111}\text{In}$ -pentetreotide scintigraphy. *J Nucl Med.* 2002;43:889–895.
34. Schillaci O, Scopinaro F, Angeletti S, et al. SPECT improves accuracy of somatostatin receptor scintigraphy in abdominal carcinoid tumors. *J Nucl Med.* 1996;37:1452–1456.

35. Lebtahi R, Cadiot G, Sarda L, et al. Clinical impact of somatostatin receptor scintigraphy in the management of patients with neuroendocrine gastroenteropancreatic tumors. *J Nucl Med.* 1997;38:853–858.
36. Chiti A, Fanti S, Savelli G, et al. Comparison of somatostatin receptor imaging, computed tomography and ultrasound in the clinical management of neuroendocrine gastro-entero-pancreatic tumours. *Eur J Nucl Med.* 1998;25:1396–1403.
37. Le Rest C, Bomanji JB, Costa DC, Townsend CE, Visvikis D, Ell PJ. Functional imaging of malignant paragangliomas and carcinoid tumours. *Eur J Nucl Med.* 2001;28:478–482.
38. Forssell-Aronsson EB, Nilsson O, Benjegard A, et al.  $^{111}\text{In}$ -DTPA-D-Phe<sup>1</sup>-octreotide binding and somatostatin receptor subtypes in thyroid tumors. *J Nucl Med.* 2000;41:636–642.
39. Benjegard SA, Forssell-Aronsson E, Waengberg B, Skanberg J, Nilsson O, Ahlman H. Intraoperative tumour detection using  $^{111}\text{In}$ -DTPA-D-Phe<sup>1</sup>-octreotide and a scintillation detector. *Eur J Nucl Med.* 2001;28:1456–1462.
40. Maina T, Nock B, Nikolopoulou A, et al. [ $^{99\text{m}}\text{Tc}$ ]Demotate, a new  $^{99\text{m}}\text{Tc}$ -based [Tyr<sup>3</sup>]octreotate analogue for the detection of somatostatin receptor-positive tumours: synthesis and preclinical results. *Eur J Nucl Med Mol Imaging.* 2002; 29:742–753.

